RSC Advances

ROYAL SOCIETY OF CHEMISTRY

www.rsc.org/advances

Cite this: DOI: 10.1039/x0xx00000x

Synthesis, crystal structure, and luminescence properties of a new microporous europium silicate: $Na_3EuSi_6O_{15}\cdot 1.47H_2O$

Wei Liu, Ying Ji, Fuyang Liu, Min Yang, Ying Wang, Xudong Zhao* and Xiaoyang Liu*

Received 00th January 2015
Accepted 00th January 2015

DOI: 10.1039/x0xx00000x

www.rsc.org/

A new microporous europium silicate, $Na_3EuSi_6O_{15}\cdot 1.47H_2O$ (denoted as **1**), was synthesized under high-temperature and high-pressure conditions, and structurally characterized by single-crystal and powder X-ray diffraction (XRD) analysis. The single-crystal XRD analysis of **1** revealed that its structure is based on corrugated silicate single layers with the composition $[Si_2O_5]$ in the *ab* plane containing 4-, 5-, 6-, and 8-rings, which are connected together by EuO_7 polyhedra via vertex oxygen atoms forming a three-dimensional framework of **1**. Compound **1** contains 4, 8-ring channels along the [100] direction and 5-, 6-ring channels along the [001] direction delimited by SiO_4 tetrahedra and EuO_7 polyhedra. The Na^+ ions are located in the free void space to balance the charge. The photoluminescence property of **1** was also investigated.

Introduction

Microporous lanthanide silicates, which contain stoichiometric amounts of framework Ln^{3+} ions, exhibit high thermal stability and tunable optical properties. They are potential candidates as optical materials and fast ion conductors.[1-5] These materials are typically synthesized in a Teflon-lined autoclave under mild hydrothermal conditions at 180-240˚C. In 1997, Rocha et al. first reported the synthesis of a microporous sodium yttrium silicate $Na_4K_2Y_2Si_{16}O_{38}\cdot 10H_2O$ (AV-1) under mild hydrothermal conditions at 503 K in Teflon-lined autoclaves.[6] Afterwards, a series of lanthanide silicates AV-n (n = 2, 5, 9, 20, 23)[7-11] have been successfully prepared under mild hydrothermal conditions. It was discovered that the flexibility of some AV-n structures can be modulated by incorporating framework lanthanide ions into the framework. The fine-tuning luminescent properties of silicates derived from the multiple Ln^{3+} ions were also investigated.

Unexpected and fascinating phases may appear when materials are subjected to high pressure (HP) because HP affects not only the structure of the flexible open framework but also the coordination environment of extraframework cations. Therefore, high-temperature (HT) and HP synthetic methods have attracted considerable attention for the synthesis of microporous lanthanide silicates that cannot be obtained under mild hydrothermal conditions. For instance, Lii et al. reported a new europium silicate, $Cs_3EuSi_6O_{15}$, which contains only tertiary $[SiO_4]$ tetrahedra. This is the second example of a 3-D silicate framework with a Si/O ratio of 2:5.[12] Later, they reported the syntheses of a series of microporous transition metals, uranium and lanthanide silicates under HP and HT hydrothermal conditions.[13-15] With continuous interest in the exploratory synthesis of lanthanide silicates and germinates under HT and HP conditions, our group has reported a number of microporous lanthanide silicates/germinates with special structures.[16-18] In 2012, we reported three new lanthanide silicates based on anionic silicate chains, layers, and frameworks prepared under HT and HP conditions.[17] In 2014, we reported two novel europium silicates based on $[Si_6O_{18}]_n^{12n-}$ cyclosilicate anions and tubular chains of SiO_4 tetrahedra prepared under HT and HP conditions.[18] In this work, we report a new europium silicate, $Na_3EuSi_6O_{15}\cdot 1.47H_2O$, the first synthetic microporous europium silicate containing seven-coordinated Eu^{3+} ions in framework. Its structure and photoluminescence property were also investigated.

Experimental

Synthesis of $Na_3EuSi_6O_{15}\cdot 1.47H_2O$

Single crystals of the title compound (denoted as **1**) were prepared from the reaction mixture of 0.12 g NaOH (Beijing Chemical Factory, 99.9%), 0.0522 g Eu_2O_3 (Aldrich, 99.9%), 0.1083 g SiO_2 (Aldrich, 99.9%) (molar ratio Na/Eu/Si = 10:1:6) in the presence of 10-11wt% distilled water, at 750 MPa, 400˚C for 48h in a piston-cylinder-type apparatus. Pressure was calibrated from melting of dry NaCl at 1050 ˚C[19] and the transformation of quartz to coesite at 500˚C[20]. The experimental temperature was monitored by a Pt100%–Pt90%Rh10% thermocouple inserted into the high-pressure cell. The starting mixture was encapsulated in a sealed platinum tube with a diameter of 5 mm and a height of 8 mm, which was separated by MgO powder from a graphite heater. The experiment was quenched before the pressure was released. The resulting colorless crystals were washed with distilled water and dried in air at 60 ˚C.

Characterizations

Powder X-ray diffraction (XRD) data were collected using a Rigaku D/Max 2550 V/PC X-ray diffractometer with graphite-monochromated Cu Kα radiation (λ = 0.15418 nm) at 50 kV

and 200 mA at room temperature. Energy-dispersive spectroscopy (EDS) analysis was carried out using an EDS system with a window attached to a JEOL JSM-6700F scanning electron microscope. Thermogravimetric analysis (TGA) was carried out on a Perkin–Elmer TGA unit in air with a heating rate of 10˚C/min. The photoluminescence (PL) spectra were obtained on a FlouroMax-4 spectrophotometer with Xe 900 (150 W xenon arc lamp) as the light source. To eliminate the second-order emission from the source radiation, a cut-off filter was used during the measurement. All spectra were recorded at room temperature.

Single-crystal Structure Determination

A suitable single crystal of 1 with dimensions of 0.12 × 0.12 × 0.04 mm^3 was selected for single-crystal XRD analysis. Intensity data were collected at the temperature of 296 K on a Bruker SMART APEX 2 micro-focused diffractometer using Mo Kα radiation (λ = 0.71073 nm) at 50kV and 0.6 mA. Data processing was accomplished with the APEX 2 processing program. Empirical absorption corrections based on symmetry equivalents were applied. The structures were solved by direct methods and refined by full-matrix least-squares techniques with the SHELXTL crystallographic software package. All heaviest atoms, Eu, Na, and Si were unambiguously located in the Fourier maps, and then O atoms were found in the subsequent difference Fourier maps. All non-hydrogen atoms were refined anisotropically. The final cycles of least-squares refinement including atomic coordinates and anisotropic thermal parameters for all atoms converged at R1 = 0.0353, wR2 = 0.0951, and S = 1.196. A summary of the crystallographic data is presented in Table 1. The selected bond lengths [Å] and angles [deg] are presented in Table S1 (Supporting Information). Atomic coordinates and equivalent isotropic displacement parameters are presented in Table S2.

Table 1 Crystal data and structure refinement for $Na_3EuSi_6O_{15}·1.47H_2O$

Empirical formula	$Na_3EuSi_6O_{15}·1.47H_2O$
Formula weight	654.95
Temperature	296(2) K
Wavelength	0.71073 Å
Crystal system, space group	Orthorhombic, *Cmm*2
Unit cell dimensions	a = 7.3669(7) Å α = 90 ˚ *b* = 30.714(3) Å β = 90 ˚ *c* = 7.0885(7) Å γ = 90 ˚
Volume	1603.9(3) $Å^3$
Crystal size	0.12 × 0.12 × 0.04 mm^3
Z, Calculated density	4, 2.704 Mg/m^3
F(000)	1247
Theta range for data collection	2.65 to 26.00 ˚.
Limiting indices	$-9 \le h \le 8, -37 \le k \le 26, -8 \le l \le 6$
Reflections collected / unique	4431 / 1524 [R(int) = 0.0249]
Completeness to theta = 26.00	99.9 %
Refinement method	Full-matrix least-squares on F^2
Data / restraints / parameters	1524 / 1 / 150
Goodness-of-fit on F^2	1.196
Final R indices [I > 2sigma(I)]	R1 = 0.0346, wR2 = 0.0947
R indices (all data)	R1 = 0.0353, wR2 = 0.0951

Results and Discussion

The powder XRD patterns of **1**, as shown in Figure 1, are consistent with the simulated XRD patterns based on the single-crystal structural analysis, indicating that they are isostructural. The intensity difference between some reflections of the experimental XRD patterns and those observed in the simulated pattern might result from preferential orientation. Table S1 in the Supporting Information displays the EDS analysis results of **1**, which is in agreement with the theoretically calculated values given by single-crystal analysis.

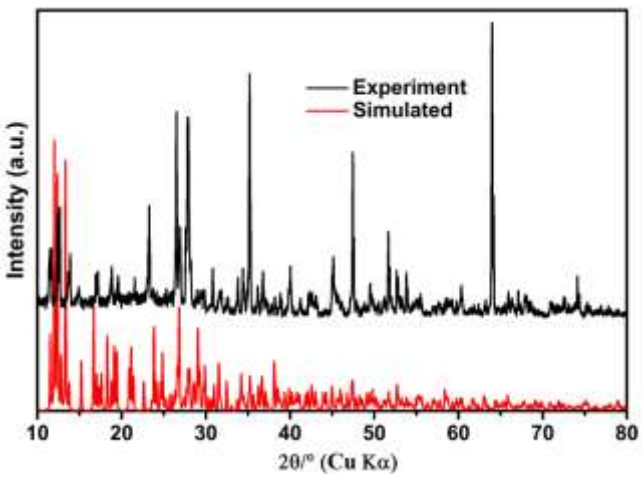

Fig.1 Simulated and experimental powder XRD patterns of **1**

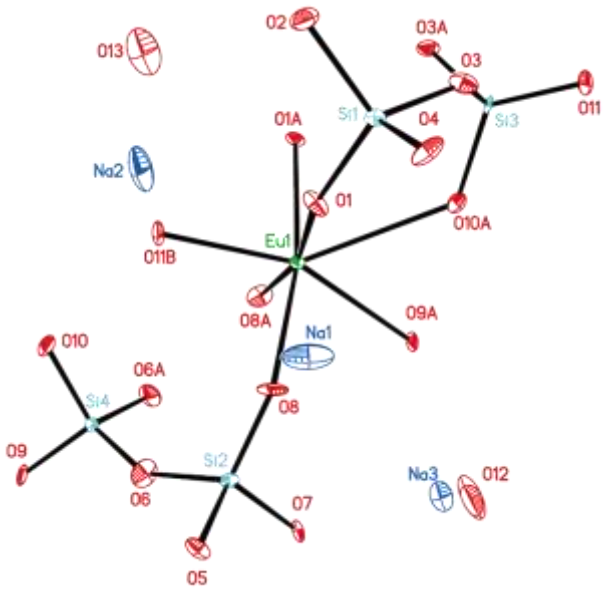

Fig.2 Thermal ellipsoid plot (50% probability) of the asymmetric unit of 1

Single-Crystal Structure of 1

Single-crystal structural analysis revealed that **1** crystallizes in the *Cmm2* space group with *a* = 7.3669(7) Å, *b* = 30.714(3) Å, and *c* = 7.0885(7) Å. Each asymmetric unit (Figure 2) of **1**

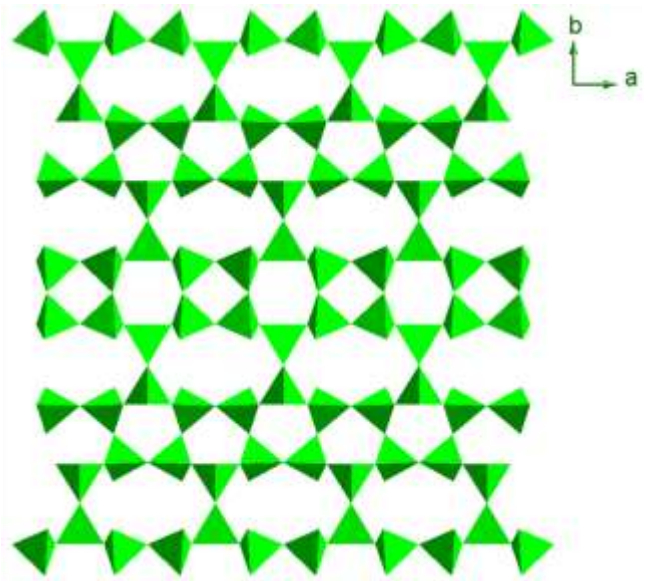

Fig.3 Polyhedral view of the silicate single layer of 1 along the [001] direction

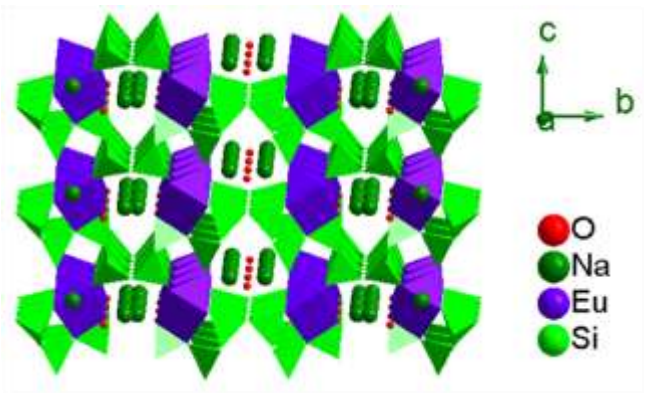

Fig.4 Polyhedral view of the open-framework structure of 1along the [100] direction. (Color code: Eu, purple; Si, bright green; Na,green; O, red)

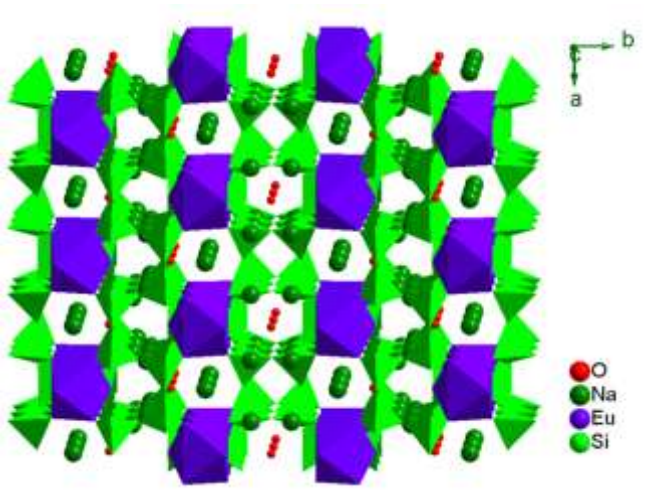

Fig.5 Polyhedral view of the open-framework structure of 1along the [100] direction. (Color code: Eu, purple; Si, bright green; Na, green; O, red).

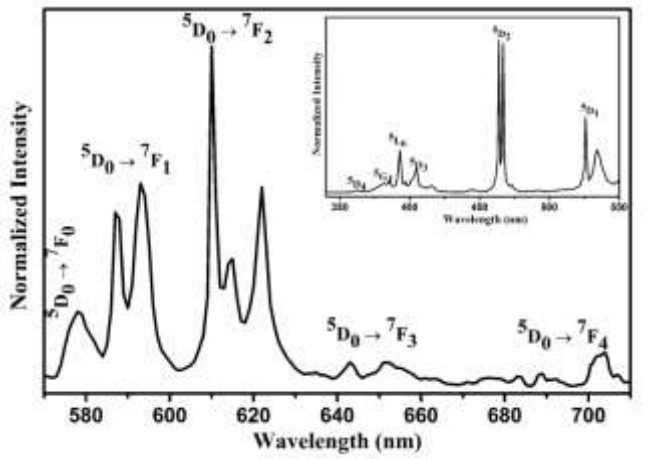

Fig.6 Room-temperature Emission and excitation spectra of **1**

contains one distinct Eu site, four symmetrically independent Si sites, and three distinct Na sites. The Eu atom is coordinated to seven bridging O atoms with the adjacent Si atoms to form a quite irregular EuO_7 polyhedron. The Eu–O bond lengths are in the range from 2.295(10) Å to 2.738(11) Å, while the O–Eu–O angles vary from 58.1(3)˚ to 175.5(3)˚. All of the Si sites are in 4-fold coordination to O atoms in tetrahedral geometry. The Si–O bond lengths are in the range of 1.571(8) –1.648(5) Å and the O–Si–O angles in the range of 102.3(5)˚–116.5(6) ˚, which are within the normal range for silicates.

The SiO_4 tetrahedra share three of their four O corners with a corner of neighboring SiO_4 group to form corrugated silicate single layers with the composition $[Si_2O_5]$ in the *ab* plane containing 4-, 5-, 6-, and 8-rings as shown in Figure 3. The $[Si_2O_5]$ layers are connected together by EuO_7 polyhedra via vertex oxygen atoms forming a three-dimensional framework of **1** (Figure 4). It contains 4, 8-ring channels along the [100] direction and 5-, 6-ring along the [001] direction (Figure 5), which are delimited by SiO_4 tetrahedra and EuO_7 polyhedra. The Na^+ ions are located in the free void space to reach charge balance. $Na(1)^+$ ions are located in the 6-rings channels along the [001] direction, while $Na(2)^+$ and $Na(3)^+$ ions are located in the 8-rings channels along the [100] direction. Seven-coordinated polyhedra of Eu^{3+} ions have been found in silicate doped with Eu^{3+} with dense structure, such as β-Ca_2SiO_4:Eu^{3+} and Y_2SiO_5:Eu^{3+}.[21-23] According to the single crystal X-ray analysis, each Eu atom is coordinated to seven neighboring O atoms forming a quite irregular EuO_7 polyhedron, which is significantly different from the reported microporous europium silicates in which Eu atoms are always six-coordinated.[12, 17, 18, 24, 25] This interesting phenomenon might be caused by the compression effects of relatively high synthesis pressure (750 MPa) on the coordinated atoms of Eu atom. More interestingly, the unusual coordination environments of Eu^{3+} ions in the structure have a significant impact on the fluorescence properties of **1**, which is also confirmed in the following fluorescence spectroscopy study. The amount of lattice water is confirmed by the TG analysis (Figure S2). The first stage of weight loss (about 5%) at the region below 250 ˚C is due to the removal of free water. The second stage of weight loss of about

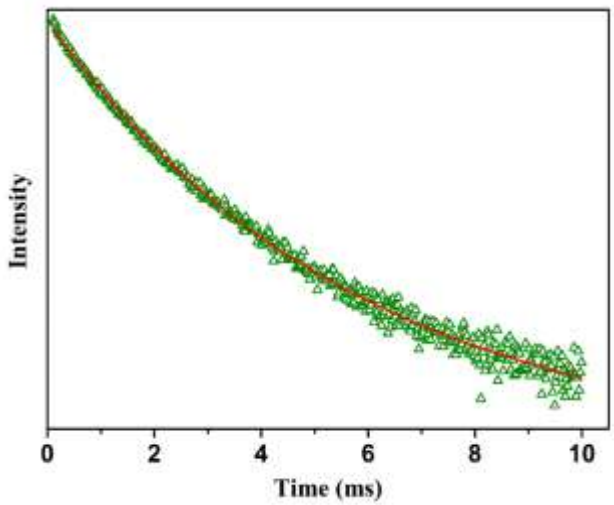

Fig.7 Single exponential fitting to the decay curve) of **1** (λem = 610 nm **)**

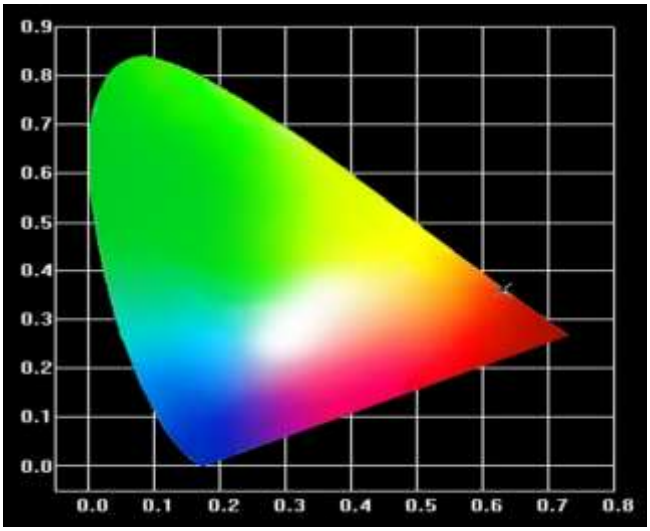

Fig.8 X and y emission color coordinates in the 1931 CIE chromaticity diagram for **1** (x = 0.639, y = 0.335; λex = 394 nm)

4.0% at temperatures of 300 to 400 ˚C is the result of liberation of lattice water (calcd. 4.04%). After 400 ˚C, no significant weight loss occurs, indicating that the sample is stable at relatively high temperature. To the best of our knowledge, compound **1** is the first synthesized microporous europium silicate with seven-coordinated Eu atoms**.**

Photoluminescence properties

Figure 6 shows the room-temperature (RT) emission and excitation spectra of **1**. The excitation spectrum, monitored at the $^5D_0 \rightarrow {}^7F_2$ transition of 610 nm, displays a series of sharp lines between 350 and 550 nm assigned to $^7F_{0\text{-}1} \rightarrow {}^5D_{4\text{-}0}$, $^5L_6$, and ^5G_J transitions of Eu^{3+}.[26, 27] The RT emission spectrum, excited at 395 nm, shows several sharp emission lines from 560 to 720 nm, which can be ascribed to emission from the first excited $^5D_0$ state to $^7F_{0\text{-}4}$ Stark levels of fundamental Eu^{3+} septet.[28, 29] Luminescence from higher excited states, such as $^5D_1$, is not detected, indicating very efficient nonradiative relaxation to the $^5D_0$ level. Only one sharp line is present in the region for $^5D_0 \rightarrow {}^7F_0$ transition. This observation indicates the presence of one Eu^{3+} local environment, which is consistent with the crystallography result that there is only one Eu^{3+} local environment in the structure. The $^5D_0 \rightarrow {}^7F_{0,\,3}$ transitions are allowed due to the ligand field effects, and the $^5D_0 \rightarrow {}^7F_1$ transitions around 594 nm have magnetic dipole (MD) characteristics. In the case of excitation at 393 nm (the $^7F_0 \rightarrow {}^5L_6$ transition), since $\Delta J = 6$, this transition and the subsequent $^5D_0 \rightarrow {}^7F_J$ (J = 2-6) emission lines would be forbidden by the usual selection rules for the Eu^{3+} species in a center of inversion.[12, 25] In other words, the $^5D_0 \rightarrow {}^7F_{2,\,4}$ transitions of **1** in the 605-625 and 685-710 nm regions would vanish when the Eu^{3+} ions are in a center of inversion in **1**. However, the integrated intensity of the $^5D_0 \rightarrow {}^7F_2$ (ED) transition is much larger than that of the $^5D_0 \rightarrow {}^7F_1$ (MD) transition in compound **1**. These results confirm the crystallographic data. The EuO_7 polyhedron in compound **1** lacks inversion symmetry since the Eu^{3+} ions are seven-coordinated. The Eu-O bond distances in the range are from 2.295(10) Å to 2.738(11)) and the EuO_7 polyhedron in **1** is strongly distorted.

The RT luminescence decay curves detected at the transition of $^5D_0 \rightarrow {}^7F_2$ (610 nm) transition of Eu^{3+} ions in **1** is shown in Figure 7 under 395 nm excitation measured at room temperature. The decay curve for Eu^{3+} emission can be well fitted by the single exponential equation: $I(t) = I_0 + A\exp(-t/\tau)$, where I and I_0 is the luminescence intensity, A the constant, t the time, τ the decay time, yielding the lifetime values of τ = 1.81 ms. These values are in good agreement with the reported values for Eu^{3+} emission.[30-32]

Figure 8 shows the x and y emission color coordinates of **1** in the 1931 CIE chromaticity diagram. It's emission color is around the red regions under 395 nm excitation, which indicates that it is a potential red phosphor.

Conclusions

A new europium silicate with novel 3-D frameworks has been synthesized using a high temperature and high pressure synthetic method. The structure of **1** is based on corrugated silicate single layers with the composition $[Si_2O_5]$ in the *ab* plane containing 4-, 5-, 6-, and 8-rings, which are linked via EuO_7 polyhedra to form a three-dimensional (3D) framework of **1.** It contains 4, 8-ring channels along the [100] direction and 5-, 6-ring along the [001] direction. The photoluminescence studies are consistent with the crystallographic results and show that **1** has strong red emission. The successful syntheses of the new europium silicates under HT and HP conditions will stimulate the study on lanthanide silicates with novel structures and special properties. Further research on the synthesis of new microporous lanthanide silicates under HT and HP conditions is underway.

Acknowledgements

This work was supported by the National Sciences Foundation of China (No.21271082, 21301066 and 21371068). and China Postdoctoral Science Foundation funded (No.801141080411).

Notes and references

State Key Laboratory of Inorganic Synthesis and Preparative Chemistry, College of Chemistry, Jilin University, 2699 Qianjin Street, Changchun, 130012, P. R. China; E-mail: liuxy@jlu.edu.cn ;

† Electronic Supplementary Information (ESI) available: [details of any supplementary information available should be included here]. See DOI:10.1039/b000000x/

1. C. Feldmann, T. Jüstel, C. R. Rond and P. J. Schmidt, *Adv. Funct. Mater.*, 2003, **13**, 511.
2. B. M. van der Ende, L. Aartsa and A. Meijerink, *Phys. Chem. Chem. Phys.*, 2009, **11**, 11081.
3. A. Dobrowolska and E. Zych, *J. Solid State Chem.*, 2011, **184**, 1707.
4. K. V. Ivanovskikh, A. Meijerink, F. Piccinelli, A. Speghini, E. I. Zinin, C. Ronda and M. Bettinelli, *J. Lumin.*, 2010, **130**, 603.
5. L. L. Han, L. Zhao, J. Zhang, Y. Z. Wang, L. N. Guo and Y. H. Wang, *RSC Adv.*, 2013, **3**, 21824.
6. J. Rocha, P. Ferreira and L. Zhi, *Chem. Commun.*, 1997, 2013.
7. D. Ananias, M. Kostova, F. A. A. Paz, A. Ferreira, L. D. Carlos, J. Klinowski and J. Rocha, *J. Am. Chem. Soc.*, 2004, **126**, 10410.
8. M. H. Kostovaa, D. Ananiasa, L. D. Carlosc and J. Rocha, *J. Alloys Compd.*, 2008, **451**, 624.
9. D. Ananias, A. Ferreira, J. Rocha, P. Ferreira, J. P. Rainho, C. Morais and L. D. Carlos, *J. Am. Chem. Soc.*, 2001, **123**, 5735.
10. A. Ferreira, D. Ananias, L. D. Carlos, C. M. Morais and J. Rocha, *J. Am. Chem. Soc.*, 2003, **125**, 14573.
11. J. Rocha, P. Ferreira, Z. Lin, P. Brandão and A. Ferreira, *J. Phys. Chem. B.*, 1998, **103**, 4739.
12. M. Y. Huang, Y. H. Chen, B. C. Chang and K. H. Lii, *Chem. Mater.*, 2005, **17**, 5743.
13. L. I. Hung, S. L. Wang, H. M. Kao and K. H. Lii, *Inorg. Chem.*, 2003, **42**, 4057.
14. F. R. Loa and K. H. Lii, *J. Solid State Chem.*, 2005, **178**, 1017.
15. C. S. Chen, R. K. Chiang, H. M. Kao and K. H. Lii, *Inorg. Chem.*, 2005, **77**, 3914.
16. W. Liu, M. Yang, Y. Ji, F. Y. Liu, Y. Wang, X. F. Wang, X. D. Zhao and X. Y. Liu, *RSC Adv.*, 2014, **4**, 26951.
17. X. Zhao, J. Li, P. Chen, Y. Li, P. Chu, X. Y. Liu, J. H. Yu and R. R. Xu, *Inorg. Chem.*, 2010, **49**, 9833.
18. W. Liu, Y. Ji, X. J. Bao, Y. Wang, B. X. Li, X. F. Wang, X. D. Zhao, X. Y. Liu and S. H. Feng, *Dalton Trans.*, 2014, **43**, 13892.
19. S. R. Bohlen, *Neues Jahrb. Mineral. Monatsh.*, 1984, **9**, 404.
20. S. R. Bohlen and A. L. Boettcher, *J. Geophys. Res.*, 1982, **87**, 7073.
21. A. Baran, J. Barzowska, M. Grinberg, S. Mahlik, K. Szczodrowski and Y. Zorenko, *Opt Mater.*, 2015, **39**, 282.
22. M. D. Drami´canin, B. Viana, Ž. Andrić, V. Djoković and A. S. Luyt, *J Alloy Compd.*, 2008, **464**, 357.
23. C. Cannas, M. Mainas, A. Musinu, G. Piccaluga, S. Enzo, M. Bazzoni, A. Speghini and M. Bettinelli, *Opt Mater.*, 2007, **29**, 585.
24. P. Brandão, A. Valente, A. Philippou, A. Ferreira, M. W. Anderson and J. Rocha, *Eur. J. Inorg. Chem.*, 2003, 1175.
25. P. Y. Chiang, T. W. Lin, J. H. Dai, B. C. Chang and K. H. Lii, *Inorg. Chem.*, 2007, **46**, 3619.
26. P. L. Chen, P. Y. Chiang, H. C. Yeh, B. C. Chang and K. H. Lii, *Dalton Trans.*, 2008, 1721.
27. Z. L. Fu, X. J. Wang, Y. M. Yang, Z. J. Wu, D. F. Duan and X. H. Fu, *Dalton Trans.*, 2014, **43**, 2819.
28. L. Kokou and J. C. Du, *J Non-Cryst Solids.*, 2012, **358**, 3408.
29. A. Feinle, F. Lavoie-Cardinal, J. Akbarzadeh, H. Peterlik, M. Adlung, C. Wickleder and N. Hüsing, *Chem Mater.*, 2012, **24**, 3674.
30. Maheshwary, B. P. Singh, J. Singh and R. A. Singh, *RSC Adv.*, 2014, **4**, 32605.
31. B. P. Singh, A. K. Parchur, R. S. Ningthoujam, A. A. Ansari, P. Singh and S. B. Raib, *Dalton Trans.*, 2014, **43**, 4779.
32. Q. G. Meng, J. Lin, L. S. Fu, H. J. Zhang, S. G. Wang and Y. H. Zhou, *J. Mater. Chem.*, 2001, **11**, 3382.